

## Poly(vinyl alcohol) as Emulsifier Stabilizes Solid Triglyceride Drug Carrier Nanoparticles in the $\alpha$ -Modification

Karin M. Rosenblatt<sup>†</sup> and Heike Bunjes<sup>\*,†,‡</sup>

*Institute of Pharmacy, Department of Pharmaceutical Technology,  
Friedrich-Schiller-Universität Jena, Lessingstrasse 8, 07743 Jena, Germany, and Institute  
of Pharmaceutical Technology, Technische Universität Carolo-Wilhelmina Braunschweig,  
Mendelssohnstrasse 1, 38106 Braunschweig, Germany*

Received June 26, 2008; Revised Manuscript Received October 8, 2008; Accepted October 14, 2008

**Abstract:** Colloidal dispersions of solid lipids are under intensive investigation as drug delivery systems. In the present study, poly(vinyl alcohol) (PVA) was tested as an alternative stabilizer for triglyceride nanoparticles. The dispersions contained 10% triglyceride (trimyrustin or tristearin) and 5% PVA and were prepared by high pressure melt homogenization. The nanoparticle dispersions were investigated for their thermal behavior and storage stability with special regard to the polymorphic transitions of the triglyceride matrix, including effects of storage temperature and the incorporation of model drugs (diazepam, ubidecarenone) using photon correlation spectroscopy, differential scanning calorimetry, X-ray diffraction, and transmission electron microscopy. The release of the model drug diazepam from a selected nanoparticle dispersion was investigated with differential pulse polarography. Triglyceride nanoparticles prepared with PVA displayed an unusually high stability of the metastable  $\alpha$ -modification depending on the type of triglyceride and the storage conditions. In tristearin nanoparticles, the  $\alpha$ -polymorph was stable for at least 9 months at refrigerator temperature and the particles exhibited a spherical shape in electron microscopic investigations. Moreover, the  $\alpha$ -form in PVA-stabilized tristearin nanoparticles seemed to be highly disordered, as it did not lead to a pronounced small-angle X-ray reflection. Storage at higher temperatures led to a transformation of the particles into the  $\beta$ -modification, which usually was accompanied by an increase in particle size. Incorporation of the two model drugs did not change the crystal modification of the particle matrix to a large extent. After dilution into a large volume of release medium, a large fraction of the model drug diazepam was released immediately but there was no further release over several hours. The high stability of PVA-stabilized tristearin nanoparticles with regard to particle size and  $\alpha$ -modification makes them suitable as a model for investigations on the influence of the polymorphic form (e.g., in comparison with nanoparticles in the more stable  $\beta$ -modification) on pharmaceutically important parameters such as drug load and drug release.

**Keywords:** Solid lipid nanoparticles;  $\alpha$ -modification; triglycerides; poly(vinyl alcohol); physico-chemical characterization; drug release

### Introduction

Submicrometer dispersions of nonpolar lipids are under intensive investigation as drug delivery systems for lipophilic drugs,<sup>1–5</sup> for example, for parenteral, especially intravenous

administration. Common matrix materials used for the nanoparticles are triglycerides, fatty acids, waxes, and cholesterol esters which are dispersed in an aqueous phase with the aid of surface active agents such as, for example, phospholipids, bile salts, poloxamers, or polysorbates. The lipid matrix of the nanoparticles can be in the liquid, liquid crystalline, or solid state. A common preparation procedure for the dispersions, especially for solid lipid nanoparticles, is the melt homogenization process, where the dispersion is prepared with high pressure homogenization at a temperature above the melting point of the lipid. The physical state of

\* Corresponding author. Mailing address: Institute of Pharmaceutical Technology, Technische Universität Carolo-Wilhelmina Braunschweig, Mendelssohnstrasse 1, 38106 Braunschweig, Germany. Telephone: (+49) 0531 3915657. Fax: (+49) 0531 3918108. E-mail: Heike.Bunjes@tu-braunschweig.de.

<sup>†</sup> Friedrich-Schiller-Universität Jena.

<sup>‡</sup> Technische Universität Carolo-Wilhelmina Braunschweig.

the particles after preparation may be different from that of the bulk lipid at room temperature, as a large supercooling effect is often observed in colloidal lipid dispersions.<sup>6–8</sup> Emulsifiers were shown to have an influence on the extent of supercooling of triglyceride nanoparticles: for example, saturated phospholipids increase the recrystallization temperature compared to unsaturated ones.<sup>9,10</sup> It is therefore necessary to verify the state of the nanoparticles after preparation, for example, with thermal investigations.

Many of the lipids used for the preparation of solid lipid nanoparticles, for example, triglycerides, are polymorphic substances. Triglycerides occur in three major crystal modifications: the metastable  $\alpha$ - and  $\beta'$ -modifications and the stable  $\beta$ -modification.<sup>11–15</sup> Since the polymorphism is

monotropic, triglycerides in the  $\alpha$ - and  $\beta'$ -modification tend to transform into the stable  $\beta$ -polymorph not only upon heating but also during storage.<sup>12,13,16</sup> The colloidal state of the particles changes not only the melting and crystallization temperature but also the polymorphic behavior of the lipids. In triglyceride nanoparticles, the transformation of the metastable  $\alpha$ - into the stable  $\beta$ -modification after crystallization is usually much faster than that in bulk triglycerides.<sup>17–19</sup> There are indications that the drug loading capacity of triglyceride nanoparticles in metastable modifications may be higher than that in the stable polymorph,<sup>20,21</sup> possibly due to their less highly ordered state. If these particles could be stabilized in the metastable  $\alpha$ -modification, the extent of drug loading might thus be increased. The possibility to prepare nanoparticles in different polymorphic forms, which are stable upon storage for a reasonable period of time, is, however, very interesting not only with regard to investigating drug loading capacity but also for the examination of drug release profiles. For example, alterations in drug release properties after the administration of solid lipid nanoparticles to skin have been attributed to polymorphic transitions of the matrix lipid.<sup>21</sup>

It has been observed that emulsifiers can affect the polymorphic transitions in bulk triglycerides<sup>13,22–24</sup> as well as in lipid nanoparticles.<sup>9,10,17,25,26</sup> For example, nanoparticles based on longer chain triglycerides emulsified with the bile salt sodium glycocholate<sup>17,25</sup> or with a mixture of saturated phospholipids and sodium glycocholate<sup>10</sup> remained in the  $\alpha$ -modification for some time.

- (1) Collins-Gold, L. C.; Lyons, R. T.; Bartholow, L. C. Parenteral emulsions for drug delivery. *Adv. Drug Delivery Rev.* **1990**, *5*, 189–208.
- (2) Benita, S.; Levy, M. Y. Submicron emulsions as colloidal drug carriers for intravenous administration: comprehensive physicochemical characterization. *J. Pharm. Sci.* **1993**, *82*, 1069–1079.
- (3) Mehnert, W.; Mäder, K. Solid lipid nanoparticles. Production, characterization and applications. *Adv. Drug Delivery Rev.* **2001**, *47*, 165–196.
- (4) Bunjes, H.; Siekmann, B. Manufacture, characterization, and applications of solid lipid nanoparticles as drug delivery systems. In *Microencapsulation*, 2nd ed.; Benita, S., Ed.; Marcel Dekker: New York, 2006; pp 213–268.
- (5) Bunjes, H.; Kuntsche, J. Supercooled smectic nanoparticles. In *Nanoparticulate Drug Delivery Systems*; Thassu, D., Deleers, M., Pathak, Y., Eds.; Informa Healthcare: New York, 2007; pp 129–140.
- (6) Dickinson E.; McClements D. J. Fat crystallization in oil-in-water emulsions. In *Advances in Food Colloids*; Dickinson, E., McClements, D. J., Eds.; Chapman and Hall: Glasgow, 1995; pp 211–246.
- (7) Bunjes, H.; Siekmann, B.; Westesen, K. Emulsions of supercooled melts. In *Submicron Emulsions in Drug Targeting and Delivery*; Benita, S., Ed.; Harwood Academic Publishers: Amsterdam, 1998; pp 175–204.
- (8) Kuntsche, J.; Westesen, K.; Drechsler, M.; Koch, M. H. J.; Bunjes, H. Supercooled smectic nanoparticles: a potential novel carrier system for poorly water soluble drugs. *Pharm. Res.* **2004**, *21*, 1834–1843.
- (9) Bunjes, H.; Koch, M. H. J.; Westesen, K. Effects of surfactants on the crystallization and polymorphism of lipid nanoparticles. *Prog. Colloid Polym. Sci.* **2002**, *121*, 7–10.
- (10) Bunjes, H.; Koch, M. H. J. Saturated phospholipids promote crystallization but slow down polymorphic transitions in triglyceride nanoparticles. *J. Controlled Release* **2005**, *107*, 229–243.
- (11) Chapman, D. Polymorphism of glycerides. *Chem. Rev.* **1962**, *62*, 433–456.
- (12) Hagemann, J. W. Thermal behavior and polymorphism of acylglycerides. In *Surfactant Science Series: Cryst. Polymorphism Fats Fatty Acids*; Garti, N., Sato, K., Eds.; Marcel Dekker: New York, 1988; pp 9–95.
- (13) Garti, N. Effects of surfactants on crystallization and polymorphic transformation of fats and fatty acids. In *Surfactant Science Series: Crystallization and Polymorphism of Fats and Fatty Acids*; Garti, N.; Sato, K., Eds.; Marcel Dekker: New York, 1988; pp 267–303.
- (14) Sato, K. Polymorphism of pure triacylglycerols and natural fats. *Adv. Appl. Lipid Res.* **1996**, *2*, 213–268.
- (15) Himawan, C.; Starov, V. M.; Stapley, A. G. F. Thermodynamic and kinetic aspects of fat crystallization. *Adv. Colloid Interface Sci.* **2006**, *122*, 3–33.
- (16) Whittam, J. H.; Rosano, H. L. Physical aging of even saturated monoacid triglycerides. *J. Am. Oil Chem. Soc.* **1975**, *52*, 128–133.
- (17) Siekmann, B.; Westesen, K. Thermoanalysis of the recrystallization process of melt-homogenized glyceride nanoparticles. *Colloids Surf., B* **1994**, *3*, 159–175.
- (18) Westesen, K.; Drechsler, M.; Bunjes, H. Colloidal dispersions based on solid lipids. In *Food Colloids: Fundamentals of Formulation*; Dickinson, E., Miller, R., Eds.; Royal Society of Chemistry: Cambridge, U.K., 2001; pp 103–115.
- (19) Schubert, M. A.; Schicke, B. C.; Müller-Goymann, C. C. Thermal analysis of the crystallization and melting behavior of lipid matrices and lipid nanoparticles containing high amounts of lecithin. *Int. J. Pharm.* **2005**, *298*, 242–254.
- (20) Westesen, K.; Bunjes, H.; Koch, M. H. J. Physicochemical characterization of lipid nanoparticles and evaluation of their drug loading capacity and sustained release potential. *J. Controlled Release* **1997**, *48*, 223–236.
- (21) Jennings, V.; Schäfer-Korting, M.; Gohla, S. Vitamin A-loaded solid lipid nanoparticles for topical use: drug release properties. *J. Controlled Release* **2000**, *66*, 115–126.
- (22) Garti, N.; Schlichter, J.; Sarig, S. Polymorphism of even monoacid triglycerides in the presence of sorbitan monostearate, studied by the DSC. *Thermochim. Acta* **1985**, *93*, 29–32.
- (23) Schlichter Aronhime, J.; Sarig, S.; Garti, N. Mechanistic considerations of polymorphic transformations of tristearin in the presence of emulsifiers. *J. Am. Oil Chem. Soc.* **1987**, *64*, 529–533.

During our investigations on the effects of emulsifiers on the properties of triglyceride nanoparticles, we became interested in the use of poly(vinyl alcohol) (PVA). This polymer is commonly applied for the stabilization of polymer nano- and microparticles.<sup>27–29</sup> It has also successfully been used as emulsifier for the preparation of cholesteryl myristate nanoparticles in the supercooled liquid crystalline smectic state and has been shown to prevent crystallization in these nanoparticles.<sup>8</sup> Its addition to phospholipid-stabilized trilaurin nanodispersions caused alterations in the polymorphic behavior of these nanoparticles with the unexpected presence of the metastable  $\beta'$ -modification some time after preparation.<sup>30</sup>

In the current study, we examined the possibility to prepare trimyristin and tristearin nanoparticles with PVA as emulsifier and characterized the resulting dispersions for their phase behavior with differential scanning calorimetry and X-ray diffraction as well as their ultrastructure with cryo- and freeze-fracture transmission electron microscopy. The effect of loading PVA-stabilized tristearin nanoparticles with the model drugs diazepam and ubidecarenone was also evaluated. Release of the drug diazepam from a selected dispersion was investigated using an electrochemical in situ method, differential pulse polarography, which has previously been shown to be suitable for drug release measurements on liposomes, cubic phase nanoparticles, emulsions of supercooled melts, and solid lipid nanoparticles.<sup>31–33</sup>

## Experimental Section

**Materials.** Tristearin (TS; Dynasan 118, Hüls/Condea, Witten, Germany) or trimyristin (TM; Dynasan 114, Hüls/

Condea, Witten, Germany) was used as matrix lipid for the nanoparticles which were emulsified with partially hydrolyzed poly(vinyl alcohol) (PVA; Mowiol 3-83, Clariant, Frankfurt/Main, Germany). The aqueous phase contained sodium azide (Sigma, Seelze, Germany) as preservative and glycerol (Caelo, Hilden, Germany) to adjust tonicity. Diazepam (Dzp) was purchased from Synopharm (Barsbüttel, Germany), and ubidecarenone (Q10) was from Kyowa Hakko Kogyo (Tokyo, Japan). Purified water was prepared by filtration and deionization/reverse osmosis (Milli RX 20, Millipore, Schwalbach, Germany).

**Methods. Preparation of the Dispersions.** The dispersions consisted of 10% triglyceride, 5% PVA, and an aqueous phase containing 0.05% sodium azide and 2.25% glycerol (w/w concentrations). Incorporated drug concentrations were 0.1% diazepam or 1% Q10. The dispersions were prepared by melt homogenization. The triglyceride was melted at  $\sim 70$  (trimyristin) or  $\sim 80$  °C (tristearin), and the drug was dissolved in the molten triglyceride for drug-containing dispersions. PVA was dissolved in the aqueous phase which was subsequently heated to the same temperature as the molten lipid. Both phases were combined at the respective temperature and prehomogenized with an ultraturrax (Ultra-Turrax T8, Ika-Werke, Staufen, Germany) for 1 min. High pressure homogenization was performed in a Microfluidizer M110S instrument (Microfluidics, Newton, MA) for 3 min at 750 bar and  $\sim 70$  °C (trimyristin) or  $\sim 80$  °C (tristearin). The resulting dispersions were allowed to cool to room temperature and usually divided into two fractions. One fraction was stored at 23 °C and one at about 5 °C (refrigerator). Usually, two or three batches of the dispersions were prepared (Table 1).

To obtain “freshly crystallized” samples, the stored dispersion was remelted by heating to about 90 °C for 10 min and subsequently the dispersion was allowed to cool to room temperature. Afterward, the dispersion was placed into the refrigerator at approximately 5 °C and further investigated after one day of cold storage (standard procedure). “Slow crystallization” was performed by cooling the melted nanoparticles quickly to 65 °C and further cooling to 23 °C with 0.5 °C/min in a thermostat. Dispersions were “rapidly cooled” by immediate transfer of a small fraction of the hot (90 °C) dispersion into a vessel which had previously been cooled to 5 °C. Slowly and rapidly cooled dispersions were characterized within less than 1 h after storage at room or refrigerator temperature, respectively.

**Particle Size Determination of the Dispersions.** Photon correlation spectroscopy (PCS) measurements were used for investigations on storage stability of the dispersions and were performed in a Zetasizer Nano ZS instrument (Malvern, Worcestershire, U.K.) at 25 °C and an angle of 173°. The dispersions were diluted with purified and particle-free water. Four measurements with 300 s each were performed, and the last three were used to calculate the  $z$ -average diameter (“particle size”) and the polydispersity index (PDI).

The particle size distribution was investigated in a laser diffractometer with PIDS (polarization intensity dif-

- (24) Schlichter Aronhime, J. Application of thermal analysis (DSC) in the study of polymorphic transformations. *Thermochim. Acta* **1988**, *134*, 1–14.
- (25) Bunjes, H.; Koch, M. H. J.; Westesen, K. Influence of emulsifiers on the crystallization of solid lipid nanoparticles. *J. Pharm. Sci.* **2003**, *92*, 1509–1520.
- (26) Kalnin, D.; Schafer, O.; Amenitsch, H.; Ollivon, M. Fat crystallization in emulsion: Influence of emulsifier concentration on triacylglycerol crystal growth and polymorphism. *Cryst. Growth Des.* **2004**, *4*, 1283–1293.
- (27) Ueda, M.; Kreuter, J. Optimization of the preparation of loperamide-loaded poly(L-lactide) nanoparticles by high-pressure emulsification-solvent evaporation. *J. Microencapsulation* **1997**, *14*, 593–605.
- (28) Bala, I.; Hariharan, S.; Kumar, M. N. V. R. PLGA nanoparticles in drug delivery: The state of the art. *Crit. Rev. Ther. Drug Carrier Syst.* **2004**, *21*, 387–422.
- (29) O'Donnell, P. B.; McGinity, J. W. Preparation of microspheres by the solvent evaporation technique. *Adv. Drug Delivery Rev.* **1997**, *28*, 25–42.
- (30) Schaal, G. Ph.D. Thesis, Friedrich-Schiller-University, Jena, Germany, 2004.
- (31) Kontoyannis, C. G.; Douroumis, D. Release study of drugs from liposomal dispersions using differential pulse polarography. *Anal. Chim. Acta* **2001**, *449*, 135–141.
- (32) Rosenblatt, K. M.; Bunjes, H. Comparison of drug release from trimyristin nanosuspensions and nanoemulsions with differential pulse polarography. *Proc. Int. Symp. Controlled Release Bioact. Mater.* **2006**, *33*, 323.

**Table 1.** Matrix Composition of the Dispersions, Storage Conditions, and PCS Particle Size Parameters (Particle Size in nm)<sup>a</sup>

lipid	storage	drug	batch	particle size/PDI					
				after preparation	6 weeks	12 weeks	24 weeks	7 months	9 months
TM	5 °C		1	139/0.13 <sup>e</sup>					
			2	139/0.13	137/0.14	156/0.23	145/0.18		138/0.13
TM	23 °C		1	154/0.33 <sup>b,e</sup>					
			2	162/0.38 <sup>b,e</sup>					
TS	5 °C		1	147/0.15 <sup>e</sup>	140/0.10	143/0.13	144/0.12		142/0.11
			2	145/0.16 <sup>c</sup>	<i>d</i>	140/0.11	160/0.23		
			3	142/0.12	143/0.13	142/0.12			
TS	23 °C		1	142/0.10 <sup>e</sup>	143/0.11 <sup>b</sup>	231/0.23	148/0.12		
TS	5 °C	Q10	1	195/0.26 <sup>c</sup>	<i>d</i>	146/0.15	148/0.13	150/0.13	
			2	140/0.13	146/0.13	146/0.12			
TS	23 °C	Q10	1	146/0.15 <sup>c</sup>	<i>d</i>	152/0.13	155/0.14		
			2	148/0.14	150/0.14	150/0.13			
TS	5 °C	Dzp	1	174/0.23 <sup>c</sup>	<i>d</i>	144/0.12	141/0.14	146/0.13	
			2	138/0.13	146/0.13	144/0.12			
TS	23 °C	Dzp	1	149/0.17 <sup>c</sup>	<i>d</i>	146/0.11	149/0.12		
			2	142/0.14	146/0.10	146/0.11			

<sup>a</sup> TM, trimyristin; TS, tristearin; Q10, ubiquinol; Dzp, diazepam. <sup>b</sup> Large particles were observed macroscopically. <sup>c</sup> No DSC measurement was performed (usually DSC measurements were performed at the same time points as the particle size measurements).

<sup>d</sup> Only DSC measurement was performed (no particle size measurement). <sup>e</sup> DSC measurement was performed within 5–7 days after preparation (commonly DSC measurements “after preparation” were performed within 1–2 days after preparation).

Dispersion batches of the same composition stored at different temperatures, which have the same batch number, were prepared in one batch and split into two fractions after preparation.

ferential scattering) technology (LS230, Beckman-Coulter, Krefeld, Germany). Eight measurements with 90 s each were performed. The particle size volume distributions were calculated with the instrumental software (version 3.29) using the Mie theory assuming a refraction index of 1.45 for the particles. Particle size measurements after preparation were performed within 1 or 2 days of storage after preparation.

**Differential Scanning Calorimetry (DSC).** About 13  $\mu$ L of the dispersions was accurately weighed into aluminum crucibles, sealed, and placed in a Pyris 1 DSC instrument (Perkin-Elmer). The dispersions were heated to 85 °C (tristearin) or 75 °C (trimyristin) with a heating rate of 10 °C/min, held at that temperature for 10 min, cooled to 0 °C (cooling rate 5 °C/min), and heated again to 85 or 75 °C (10 °C/min), respectively. The curves shown in the figures are normalized for the weight of the samples.

DSC investigations were performed at the same time points as the PCS measurements shown in Table 1 unless otherwise noted. As several batches were investigated, the enthalpy values displayed in the figures reflected results from a single batch or the mean of 2–3 batches (Table 1). Since the tristearin content of the S100-3/SGC-stabilized dispersion differed distinctly from that of the PVA-containing dispersions (see caption to Figure 5), the enthalpy values for this dispersion were converted in such a way that they reflect the values expected for a dispersion with the same tristearin content as the PVA-stabilized dispersions.

**Transmission Electron Microscopy (TEM). Cryo-Preparation.** A few microliters of undiluted dispersion was placed on a holey grid (Quantifoil, Germany), and excess liquid was removed with filter paper. The sample was cryofixed by rapid immersion into liquid ethane cooled to –170 to –180 °C in a cryobox (Carl Zeiss NTS GmbH, Oberkochen, Germany). Excess ethane was removed by blotting in the cold. The frozen sample was transferred with a cryotransfer system (Gatan 626-DH) into the precooled cryoelectron microscope (Philips CM 120) operated at 120 kV and viewed under low-dose conditions.

**Freeze-Fracture Preparation.** A few microliters of the dispersion was placed between two sandwich copper profiles as used for propane jet freezing. The samples were manually frozen by plunging into a 1:1 mixture of liquid ethane and propane cooled by liquid nitrogen. Freeze-fracturing and replication were performed in a freeze-fracture unit BAF 400T (BAL-TEC, Balzers, Liechtenstein) at –140 °C and  $2 \times 10^{-7}$  mbar without etching. Platinum of 2 nm thickness was evaporated under an angle of 35° for shadowing of the samples followed by perpendicular evaporation of about 20 nm carbon for replica stabilization. Replicas were mounted onto electron microscopic grids (mesh 400), treated with pure ethanol, cleaned in chloroform/methanol (2:1 v/v), and investigated in a transmission electron microscope CEM 902A (Zeiss, Oberkochen, Germany), operated at 80 kV.

**X-ray Diffractometry.** Small- and wide-angle X-ray diffractograms were recorded in a capillary sample holder at 5 °C for 1 h with a SWAX camera based on a Kratky collimator system (Hecus M. Braun, Optical Systems GmbH, Graz, Austria) mounted on an Iso-DebyeFlex 3003 60 kV generator (Seifert-FPM Freiberg, Germany) with an X-ray

- (33) Rosenblatt, K. M.; Douromis, D.; Bunjes, H. Drug release from differently structured monoolein/poloxamer nanodispersions studied with differential pulse polarography and ultrafiltration at low pressure. *J. Pharm. Sci.* **2007**, *96*, 1564–1575.



tube (copper anode) FK 61-04  $\times$  12 and equipped with two position sensitive detectors (PSD-50M, M. Braun, Garching, Germany). Small-angle X-ray diffractograms were de-smearred, and small- and wide-angle X-ray diffractograms were smoothed for evaluation and presentation.

**Drug Release.** The release of diazepam was investigated with differential pulse polarography using a Metrohm 746 VA Trace Analyzer and a 747 VA Stand (Switzerland). A total of 10 mL of the release medium (Tris buffer, 10 mM, pH 7.4, containing 50 mM NaCl) was purged with nitrogen for 5 min, 100  $\mu$ L of the dispersion was added, the mixture was purged for another 30 s with nitrogen, and the measurement was started. The potential sweep for diazepam was from  $-700$  to  $-1450$  mV, with the peak position of diazepam being detected around  $-1100$  mV. The voltage amplitude was 50 mV (step time 0.3 s), measuring time 20 ms, and pulse time 40 ms. Recording of one sweep took approximately 20 s. The calculation of diazepam concentration was done using a calibration curve based on diazepam standard solutions. The measurements were performed at 23  $^{\circ}$ C, and the release was measured in triplicate.

**Analytical Characterization.** For selected dispersions, the triglyceride and/or the drug content was determined. The diazepam content of the dispersions was analyzed using high performance liquid chromatography (HPLC) (Beckman-Coulter, Gold System with diode array UV detector, 32Karat ver. 5.0 software, Krefeld, Germany) with a LiChrospher RP18, 5  $\mu$ m column (Macherey-Nagel, Switzerland), 125 mm  $\times$  3 mm. The mobile phase was a mixture of acetonitrile/water (50/50 v/v), and the flow rate was 1 mL/min. For sample preparation, 100  $\mu$ L of the dispersion was diluted with 5 mL of tetrahydrofuran and 2 mL of acetonitrile was added. The dilution was concentrated by aerating with nitrogen to precipitate the lipid. The sample was filtered through a glass fiber filter (Whatman, Dassel, Germany, Gf/C, nominal pore size 1.2  $\mu$ m), the filter was washed with acetonitrile, and acetonitrile was added to the filtrate up to 10.0 mL. Detection of diazepam was done at 254 nm. The recovery rate (96.0%) of the sample preparation procedure was determined in the same way with an unloaded dispersion which was spiked with different diazepam concentrations.

The amount of drug released from the dispersion was related to the real drug content determined with HPLC. The errors were calculated via error propagation including the errors of the release curves, the HPLC determination, and the recovery rate for the HPLC determination.

For the determination of the drug content in the water phase, a homemade ultrafiltration cell with a regenerated cellulose membrane (molecular weight cutoff 100 000 Da, diameter 25 mm) (Millipore) was used. About 1 mL of the dispersion was filtered, and the first droplets were discarded. The drug content was analyzed with HPLC, and the values were corrected by the drug adsorption to the membrane as described previously.<sup>33</sup>

Tristearin content was also determined with HPLC (BeckmanCoulter, Gold System, 32Karat ver. 5.0 Software, Krefeld, Germany). The column was a LiChrospher 100

RP18, 5  $\mu$ m (Merck, Germany), 250 mm  $\times$  4 mm kept at 30  $^{\circ}$ C. An evaporative light scattering detector (ELSD) (Alltech Varex MKIII ELSD) was used. The mobile phase, corresponding tube temperature, and the nitrogen gas flow of the ELSD were THF/ACN 60/40, 88  $^{\circ}$ C, 2.30 slpm, respectively. All concentrations were v/v; the flow rate was 1 mL/min.

For sample preparation, 100  $\mu$ L of the dispersions was diluted with a mixture of THF/ACN (90/10 v/v) and filtered with a glass fiber filter (Whatman, Dassel, Germany, Gf/C, nominal pore size 1.2  $\mu$ m), the filter was washed with the solvent, and the solvent was added to the filtrate up to 10.0 mL. The recovery rate (96.8%) was determined in the same way with an aqueous PVA (5%) solution spiked with lipid solutions in THF in different concentrations. All values were corrected with the recovery rate.

## Results

**Characterization of Drug-Free Dispersions and Stability during Storage.** Nanoparticles stabilized with PVA had a milky white appearance and a PCS particle size usually between about 140 and 165 nm (Table 1).

According to laser diffractometry (Figure 1), the mean particle size of the dispersions was between 110 and 120 nm, except for the trimyristin dispersion stored at room temperature, in which it was about 380 nm. This dispersion contained a large fraction of micrometer-sized particles and also macroscopically detectable particles.

During heating in DSC investigations (Figure 1), cold-stored trimyristin nanoparticles displayed a large melting signal of the  $\alpha$ -modification at 32  $^{\circ}$ C (onset  $\sim$ 30  $^{\circ}$ C) followed by an exotherm (presumably corresponding to the recrystallization of molten particles) and a second endothermic peak reflecting the melting of the  $\beta$ -modification ( $\sim$ 54  $^{\circ}$ C, onset  $\sim$ 50–51  $^{\circ}$ C). The  $\beta$ -endotherm was distinctly larger than the preceding exotherm, indicating that a fraction of particles was already in the  $\beta$ -form before heating. However, only a reflection of the  $\alpha$ -modification was observed in wide-angle X-ray diffractograms of a freshly crystallized sample (Figure 2).

In the heating curve of the trimyristin nanoparticles stored at room temperature, a small melting peak of the trimyristin  $\beta$ -modification was detected (Figure 1). The melting enthalpy of this transition corresponded to roughly 15% of the melting enthalpy expected for the whole trimyristin content of this sample, indicating that the majority of the dispersed triglyceride remained in the supercooled liquid state. The existence in this state is the common situation for melt-homogenized trimyristin nanoparticles stored at room temperature due to the large supercooling effect in the colloidal particles.<sup>7,20,34,35</sup> Also for the sample under investigation

(34) Bunjes, H.; Westesen, K.; Koch, M. H. J. Crystallization tendency and polymorphic transitions in triglyceride nanoparticles. *Int. J. Pharm.* **1996**, 129, 159–173.

(35) Bunjes, H.; Koch, M. H. J.; Westesen, K. Effect of particle size on colloidal solid triglycerides. *Langmuir* **2000**, 16, 5235–5242.

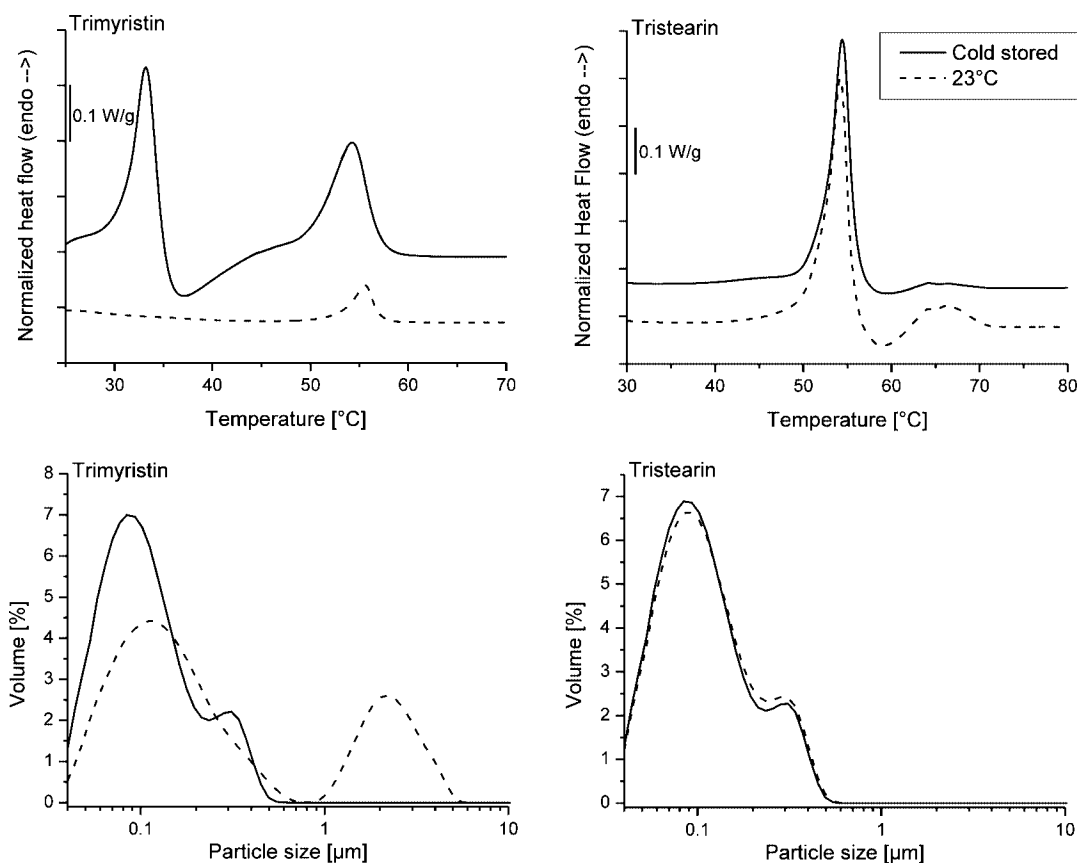


**Figure 1.** (Top) DSC heating curves of trimyristin (left) and tristearin (right) nanoparticles after preparation stored at ~5 °C (solid line) or at 23 °C (dashed line). DSC measurements were done within 5–7 days after preparation. The curves are displaced along the ordinate for better visualization. (Bottom) Particle size distributions of trimyristin (left) and tristearin (right) dispersions (laser diffractometry, 3–4 days after preparation).

here, the crystallization onset temperature was detected around 11 °C in DSC cooling runs, reflecting a large supercooling tendency. The occurrence of a non-negligible fraction of crystalline trimyristin in the room temperature stored trimyristin dispersions can very likely be attributed to the microparticulate fraction (in which the supercooled state is less stable) detected by laser diffractometry. Due to this instability phenomenon, room temperature stored trimyristin dispersions were not investigated any further.

The heating curve of the cold-stored tristearin nanoparticles displayed a large endotherm around 54 °C (onset ~52 °C) which points to the presence of  $\alpha$ -polymorph. Only a very small exothermic peak and an endothermic melting peak of the  $\beta$ -polymorph, which were of approximately the same size, could be detected. This indicates that the small fraction of  $\beta$ -polymorph was not originally present in the sample but resulted from recrystallization after melting of the  $\alpha$ -modification. In wide-angle X-ray diffractometry, only the reflection of the  $\alpha$ -form was detected (Figure 2).

Also the tristearin sample stored at room temperature displayed a pronounced  $\alpha$ -melting signal in DSC. The following exotherm and the  $\beta$ -endotherm were again of roughly the same size but larger than those of the cold-stored tristearin dispersion.

The crystallization onset temperature upon cooling was about 34 °C for the tristearin dispersions which—as the value

obtained for the trimyristin dispersion—is in good agreement with the value observed for emulsifiers with no special effect on the crystallization temperature.<sup>10</sup>

During further cold storage (up to 9 months) of the trimyristin dispersion, only small changes in the size of the  $\alpha$ -melting endotherm, the exotherm, and the  $\beta$ -melting endotherm were observed (Figure 2). Small differences observed for the enthalpy especially of the  $\alpha$ -polymorph might be attributed to difficulties in evaluation of the peak size, since heating was started at 20 °C and no stable baseline was reached prior to the onset of the endothermic signal. Additionally, the exotherm overlaps the melting endotherm of the  $\alpha$ -polymorph, which also complicates the exact evaluation of both peak sizes. The PCS particle size did not remarkably change over storage (Table 1). Wide-angle X-ray diffractograms revealed the single strong reflection of the  $\alpha$ -modification<sup>11</sup> for both a freshly crystallized (1 day of cold storage) and a cold-stored dispersion (9 months storage). The small-angle diffractograms displayed a strong reflection as well, with slightly higher intensity for the stored dispersion.

Also for the cold-stored tristearin dispersion, the DSC heating curves as well as the particle size did not change notably over storage time (Table 1, Figure 2). In contrast to the trimyristin dispersion, there was only a small, broad reflection in the small-angle X-ray diffractogram (Figure 2), indicating a low order of the triglyceride molecular layers.

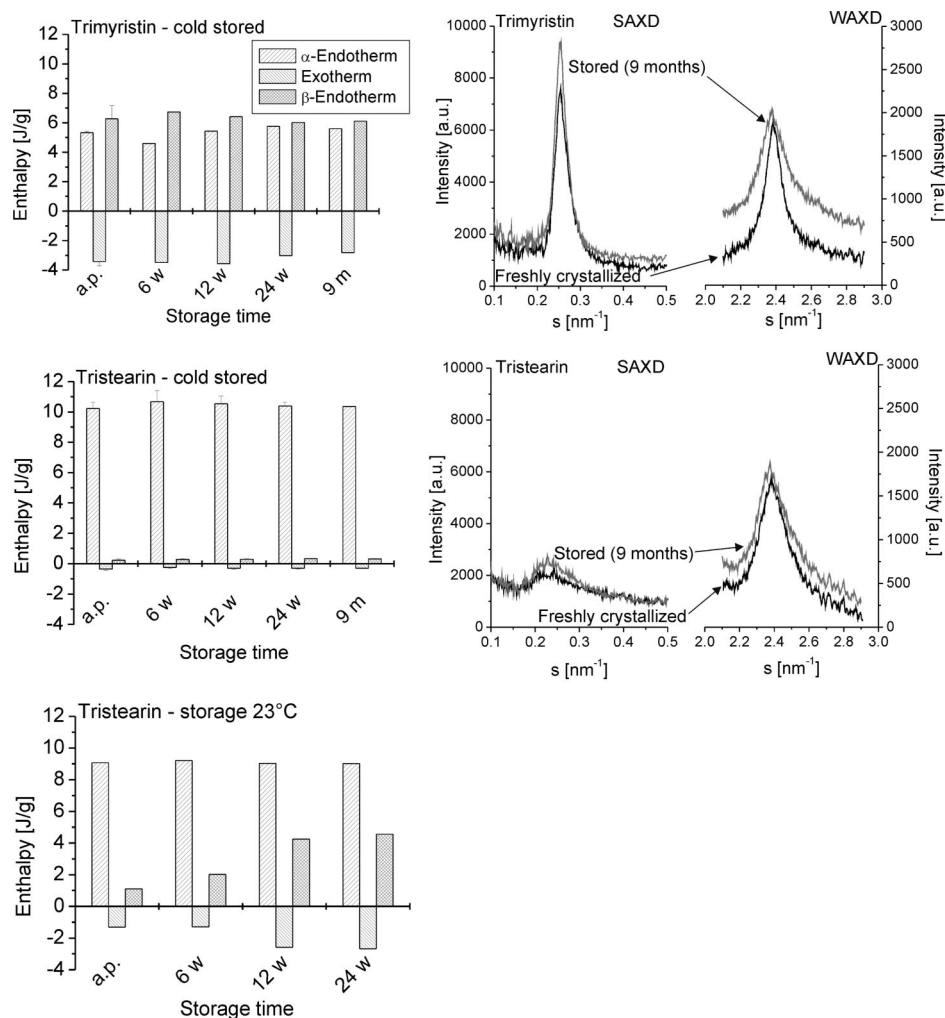


**Figure 2.** Evolution of thermal behavior and structure of the particles during storage. (Left) Enthalpy of the endothermic and exothermic signals obtained from DSC heating runs (a.p., after preparation; w, weeks; m, months) ( $n = 1-3$ , see Table 1). (Right) Small- and wide-angle X-ray diffractograms of freshly crystallized and stored samples. The curves were displaced along the ordinate for better visualization.

The size of this reflection increased only very slightly during storage and remained much smaller than that of the trimyristin dispersion. The wide-angle reflection of the  $\alpha$ -modification was, however, clearly visible and roughly comparable in size to that of the trimyristin dispersion for both the cold-stored and the freshly crystallized tristearin dispersion.

It should be mentioned that the DSC investigations shown in Figure 2 were performed after preparation, whereas the X-ray measurements were performed with freshly crystallized dispersions. DSC investigations of the freshly crystallized samples were, however, similar to those obtained after preparation of the dispersions.

The size of the  $\beta$ -endotherm in the heating curves of the room temperature stored tristearin dispersion increased over storage time. Additionally, the size of the exotherm increased. As large particles were observed visually after 6 weeks of storage and a larger PCS particle size (indicating instability of the sample) was obtained after 12 weeks, this dispersion was not investigated with X-ray diffractometry.

**Storage at Elevated Temperatures.** To further examine the stability of the  $\alpha$ -modification in the nanoparticles,

previously cold-stored dispersions were stored at different temperatures below the melting point of the  $\alpha$ -modification. The trimyristin dispersion was examined at 23 °C, and tristearin at 23, 37, and 45 °C (Figure 3).

For trimyristin nanoparticles stored at 23 °C (i.e.,  $\sim 9$  °C below the observed melting temperature of the  $\alpha$ -form), a large decrease of the  $\alpha$ -endotherm and an increase of the  $\beta$ -endotherm were already apparent after 1 day. After 12 weeks of storage, the  $\alpha$ -endotherm had completely disappeared from this sample. Transformation into the  $\beta$ -modification was confirmed by X-ray diffraction (performed after 7 months of storage). The small-angle reflection of the particles in the  $\alpha$ -modification corresponded to a long spacing of about 3.95 nm, which is slightly lower than a literature value of 4.12 nm<sup>11</sup> for trimyristin; the  $\beta$ -long spacing was at 3.56 nm (literature: 3.58 nm<sup>11</sup>). The changes in polymorphic form were accompanied by an increase in particle size which was comparatively large after 12 weeks of storage (z-average diameter/PDI: 200 nm/0.19).

Tristearin nanoparticles stored at 45 °C (i.e.,  $\sim 9$  °C below the  $\alpha$ -melting temperature) also displayed a distinct decrease

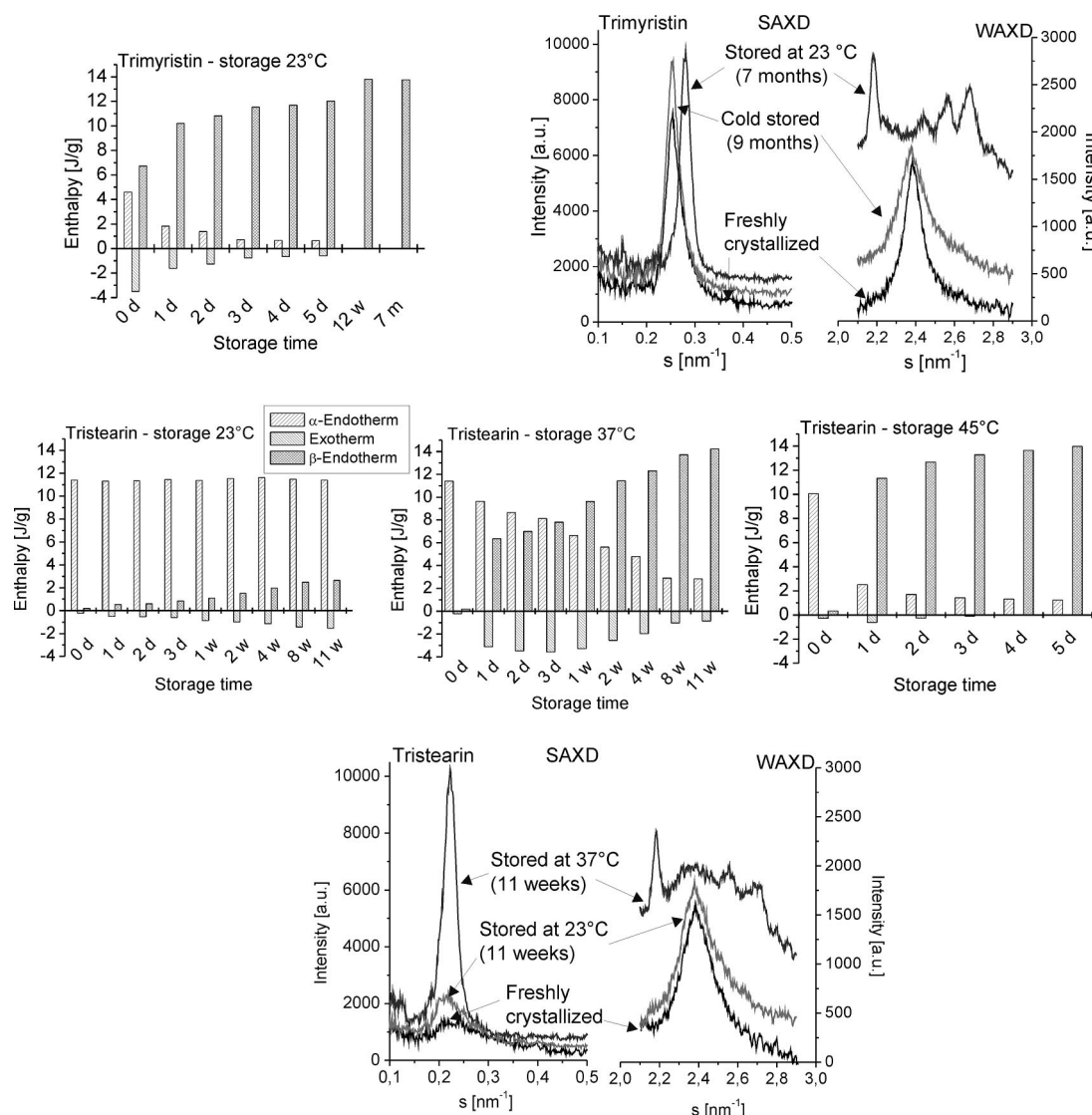


**Figure 3.** Influence of storage temperature on the thermal behavior (size of signals in the heating curve in DSC) of trimyristin and tristearin nanoparticles at different elevated temperatures and corresponding X-ray small- and wide-angle diffractograms (displaced along the ordinate for better visualization). Please note the different time scales in the graphs showing enthalpy versus time. (Top) Trimyristin (left) DSC and (right) X-ray diffractometry. (Middle) Tristearin DSC. (Bottom) Tristearin X-ray diffractometry.

of the  $\alpha$ -endotherm already after 1 day. The particle size as determined by PCS increased markedly (z-average > 200 nm after 1 day), and after a few days large particles were observed macroscopically. Storage at 37 °C also led to an increase of the exotherm and  $\beta$ -endotherm as well as to a decrease of the  $\alpha$ -endotherm already after 1 day, but the changes were much smaller than those upon storage at 45 °C. The decrease of the  $\alpha$ -endotherm and the increase of the  $\beta$ -endotherm continued over a further 11 weeks of storage. The exotherm, however, increased over 3 days and then decreased during further storage. After about 1 week, the enthalpy of particles in the  $\beta$ -modification originally present in the sample was larger than that of the  $\alpha$ -modification. However, even after 11 weeks, a fraction of particles in the  $\alpha$ -modification remained. At this storage temperature, the particle size increased distinctly after 2 weeks of storage and macroscopically large particles were detected.

In tristearin nanoparticles stored at 23 °C, the proportion of the fraction of  $\alpha$ - and  $\beta$ -polymorphs changed only slowly. After 11 weeks, still a large amount of the particles was in the  $\alpha$ -modification. The slight increase in the fraction of particles in the  $\beta$ -modification during storage was accompanied by an increase in the size of the exotherm. This means that the fraction of particles in the  $\alpha$ -form which recrystallize after melting increased and thus contributed to the larger fraction of  $\beta$ -polymorph. In this sample, the particle size and the PDI remained stable over the whole period of storage.

X-ray investigations of the tristearin dispersions stored at 23 and 37 °C for 11 weeks were compared with a freshly crystallized sample (1 day in the refrigerator). The wide-angle diffractograms revealed the typical reflections of the  $\alpha$ -modification for the freshly crystallized dispersion and the dispersion stored at room temperature, whereas the



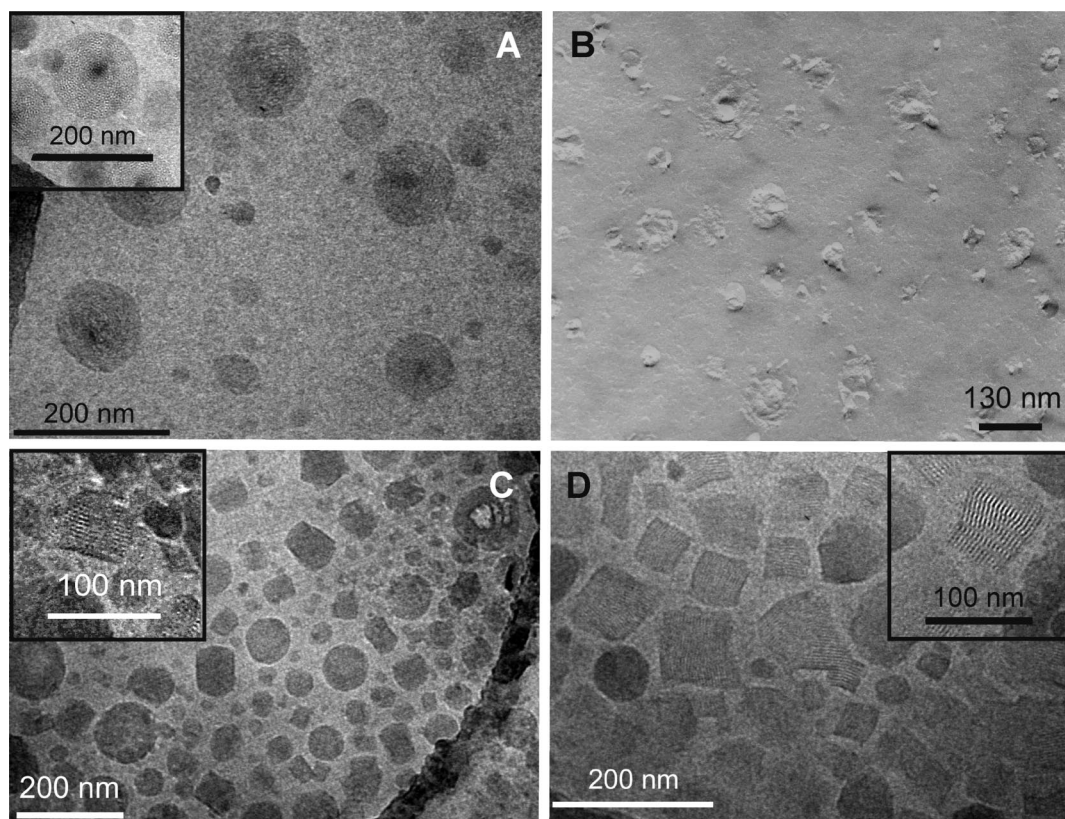


**Figure 4.** Transmission electron micrographs. (A) Tristearin nanoparticles (cold-stored for 7 weeks, cryo-preparation), (B) tristearin nanoparticles (cold-stored for 6 months, freeze-fracture preparation), (C) trimyristin nanoparticles (cold-stored for 7 weeks, cryo), and (D) trimyristin nanoparticles (6 days storage at 23 °C, cryo). Insets in micrographs obtained by cryo-preparation: filtered micrographs (fast Fourier transformation).

dispersion stored at 37 °C additionally displayed reflections of the  $\beta$ -modification. The small-angle reflection was somewhat more intense for the dispersion stored at 23 °C compared to the freshly crystallized sample but still pointed to a low degree of order of the underlying crystal structure. In contrast, the dispersion stored at 37 °C led to a very strong small-angle reflection caused by a high degree of long-range order of the triglyceride layers. The spacing of the small-angle reflection of the dispersion stored at 37 °C (4.49 nm) is close to the  $\beta$ -polymorph literature value of 4.50 nm.<sup>11</sup> For the freshly crystallized dispersion and the dispersion stored at room temperature, it is very difficult to determine the exact position of the small-angle reflection due to its small size. At least, the spacing of the dispersion stored at room temperature seems to be larger than that of the  $\beta$ -polymorph, as expected for the  $\alpha$ -form (literature value 5.06 nm).<sup>11</sup>

**Electron Microscopy.** Tristearin nanoparticles in the  $\alpha$ -modification (cold-stored) appeared as circular structures with a denser center in cryoelectron microscopy (Figure 4A). An onionlike layered structure, which was previously observed for nanoparticles stabilized with saturated phospholipids in the  $\alpha$ -modification<sup>36</sup> could not unambiguously

be detected, even not after application of a FFT (fast Fourier transformation)-filter. The particles were extremely sensitive to the electron beam and started to “bubble” upon longer observation. In freeze-fracture electron microscopy, cold-stored tristearin particles appeared as circular particles as well (Figure 4B). The interior of the particles revealed by some cross-fractured particles did not display a clearly layered structure. The micrographs of the cold-stored trimyristin nanoparticles (Figure 4C) also displayed circular or sometimes polygonal structures. In contrast to the tristearin particles, a core of higher density could not be observed in these particles. Besides these circular structures, a lot of rectangular particles could be found, which were in some cases smaller than the circular structures. A few of the rectangular particles seem to contain a layered structure.

The cold-stored trimyristin sample which had subsequently been kept at 23 °C for 6 days and thereby transformed into the  $\beta$ -modification mainly contained more or less irregular angular particles (Figure 4D). These particles clearly exhibited a layered structure with several imperfections.

**Influence of the Crystallization Procedure.** The standard procedure to cool the dispersions after preparation or after remelting the dispersions at 90 °C (“freshly crystallized dispersion”) was passive cooling to room temperature. Afterward, the dispersions were placed into the refrigerator

(36) Bunjes, H.; Steiniger, F.; Richter, W. Visualizing the structure of triglyceride nanoparticles in different crystal modifications. *Langmuir* **2007**, *23*, 4005–4011.

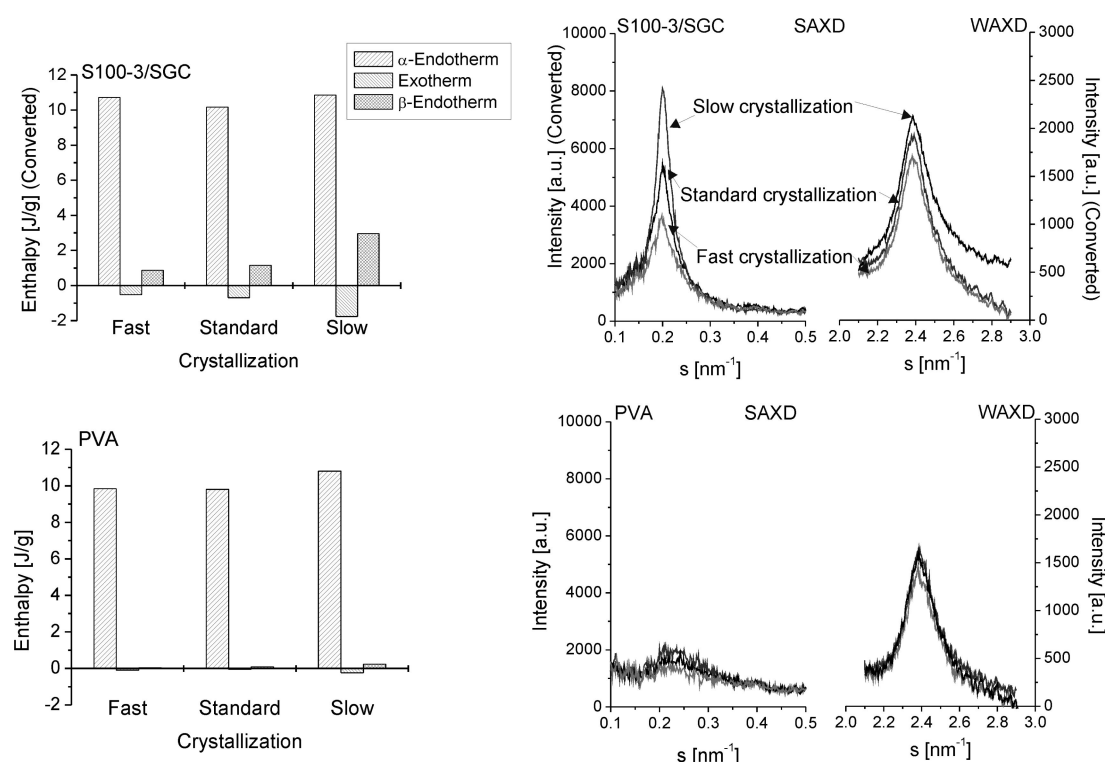


**Figure 5.** (Left) Influence of the crystallization procedure on the thermal behavior of a tristearin dispersion stabilized with saturated phospholipids (S100-3) and sodium glycocholate (SGC) (top) and a PVA-stabilized tristearin dispersion (bottom). Corresponding X-ray diffractograms are shown on the right. The curves of the S100-3/SGC-containing dispersion are converted to the triglyceride content of the PVA-stabilized dispersion as the real triglyceride contents as determined by HPLC differed significantly: S100-3/SGC-containing dispersion,  $132.16 \pm 0.88$  mg/mL; PVA-dispersion,  $76.80 \pm 1.03$  mg/mL.

and further investigated after 1 day of cold storage. To study the impact of the crystallization procedure on the amount and structure of the  $\alpha$ -modification, the dispersions were additionally crystallized in a slow or fast way. For comparison, a previously described<sup>10,36</sup> tristearin (10%) dispersion stabilized with a combination of saturated soy bean phospholipid (Lipoid S100-3) (S100-3; 2.4%) and sodium glycocholate (SGC; 0.6%) was investigated additionally.

Small-angle X-ray diffraction revealed a distinct influence of the cooling conditions on the height of the peak for the dispersion stabilized with saturated phospholipid/sodium glycocholate (Figure 5). It was lowest for the rapid crystallization, intermediate for the standard crystallization, and highest for the slow crystallization. Only slight differences were visible in the wide-angle diffraction pattern, in which each dispersion showed an  $\alpha$ -reflection of similar intensity. In DSC, an increasing size of the exotherm and the  $\beta$ -endotherm was observed from fast over standard to slow crystallization.

Irrespective of the crystallization procedure, the PVA-stabilized tristearin dispersions were also in the  $\alpha$ -modification according to wide-angle X-ray investigations. Taking into consideration the differences in tristearin content of S100-3/SGC- and PVA-stabilized dispersions (Figure 5 contains correspondingly converted values for the DSC and X-ray curves of the S100-3/SGC-stabilized dispersion), the size of the wide-angle reflections was not remarkably different from that of the

S100-3/SGC-stabilized dispersion. PVA-stabilized tristearin dispersions revealed, however, far less pronounced small-angle X-ray reflections. Differences in the height of the reflections between the crystallization procedures were only marginal (same order as in the S100-3/SGC-stabilized dispersion). Furthermore, only minor differences of the sizes of the DSC signals were observed among the differently crystallized dispersions with a slightly larger size of the  $\alpha$ -endotherm of the slowly crystallized nanoparticles.

**Drug Loading.** The effect of drug loading on the stability of the  $\alpha$ -form upon storage in the cold and at room temperature was investigated with two different lipophilic model drugs: ubidecarenone (Q10) and diazepam. The DSC heating curve of the cold-stored diazepam-loaded (0.1%) tristearin dispersion was very similar to that of the unloaded one (Figure 6). Almost the whole fraction of the dispersion was in the  $\alpha$ -modification. An exotherm and  $\beta$ -endotherm were hardly noticeable. Storage over 7 months did not change the DSC melting behavior remarkably. X-ray diffractometry revealed comparably low ordering in the small-angle range as for unloaded tristearin dispersions. The differences between freshly crystallized particles and cold-stored particles were even smaller than those in unloaded nanoparticles. The wide-angle X-ray diffractograms displayed the typical reflection of the  $\alpha$ -modification. The particle size did not change during storage (Table 1).

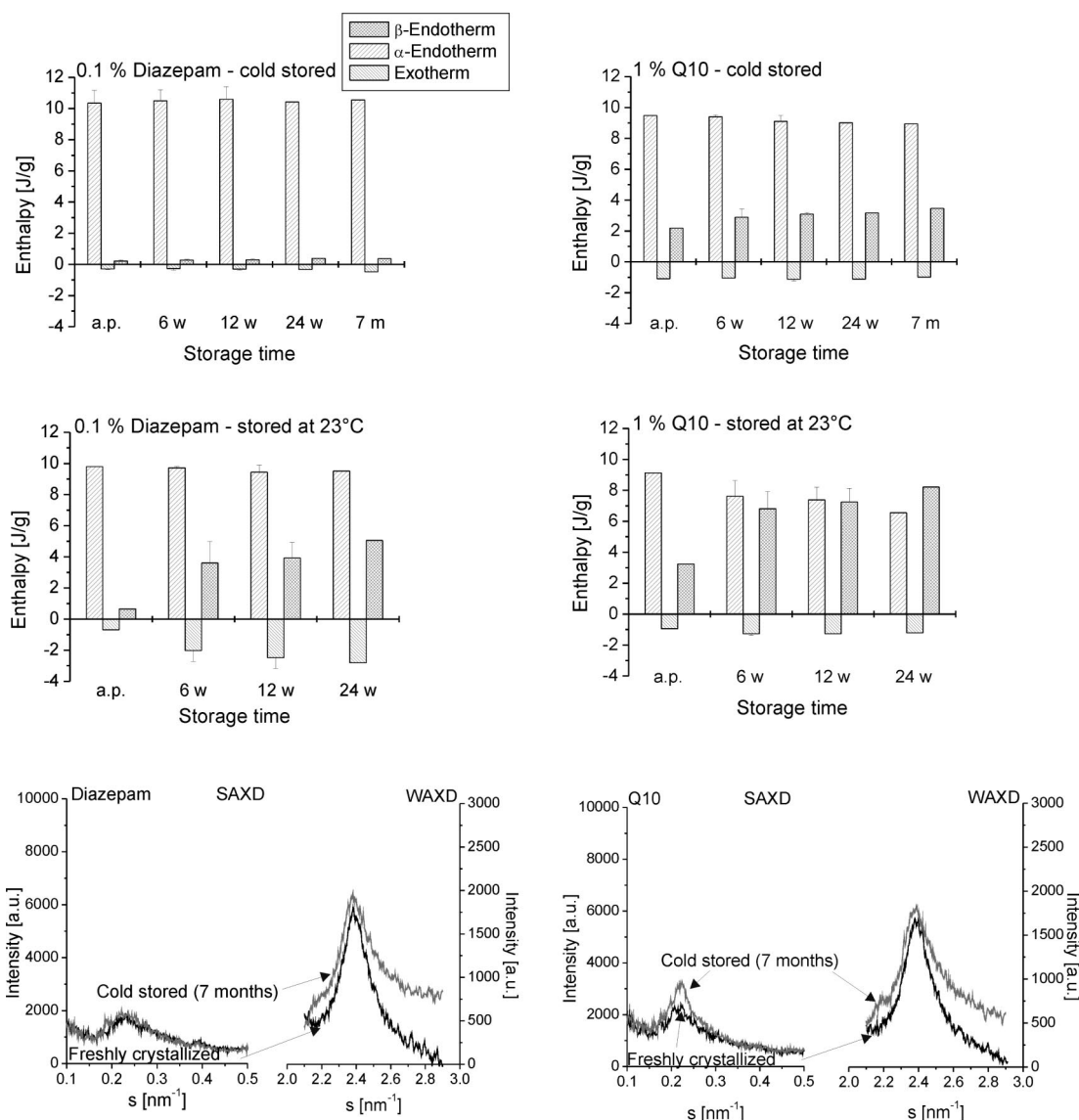


**Figure 6.** Drug-loaded tristearin nanoparticles: influence of storage temperature and time investigated with DSC. Comparison of a freshly crystallized drug-loaded tristearin dispersion and a dispersion cold-stored for 7 months with X-ray diffractometry. (Left) Diazepam- and (right) Q10-loaded dispersion. (Top and middle) DSC enthalpies of cold and room temperature stored dispersions, and (bottom) X-ray diffractograms.

The diazepam-loaded tristearin dispersion stored at room temperature exhibited a small exotherm and  $\beta$ -endotherm after preparation. During storage, the size of these signals increased markedly, whereas the size of the  $\alpha$ -endotherm did not decrease distinctly. The particle size remained constant for 24 weeks. Compared to the unloaded sample stored at room temperature, no large differences could be observed except for a larger increase of the exotherm and the  $\beta$ -endotherm after 6 weeks.

Q10 (incorporated at a concentration of 1% in the dispersion), which is known to accelerate polymorphic transitions of triglycerides into the stable  $\beta$ -modification,<sup>37</sup> increased the size of the endothermic  $\beta$ -melting signal in

cold-stored tristearin dispersions already after preparation compared to an unloaded dispersion, but there was still a distinct peak of the  $\alpha$ -modification. During cold storage, the most apparent change was the increase in the size of the  $\beta$ -endotherm, whereas that of the  $\alpha$ -endotherm decreased only slightly and the size of the exotherm almost remained constant. Compared to the unloaded and the diazepam-loaded dispersion, the onset of the  $\alpha$ -melting endotherm of the Q10-loaded dispersion was roughly 2 °C lower ( $\sim 50$  °C). Also, the crystallization onset during cooling was lower ( $\sim 32$  °C) compared to the unloaded ( $\sim 34$  °C) and the diazepam-loaded dispersion ( $\sim 33$  °C). Wide-angle X-ray diffraction revealed reflections of the  $\alpha$ -polymorph for both the freshly crystallized and the dispersion stored for 7 months. A small reflection of the  $\beta$ -polymorph can, however, be presumed in the diffractogram of the stored dispersion. The small-angle

(37) Bunjes, H.; Drechsler, M.; Koch, M. H. J.; Westesen, K. Incorporation of the model drug ubidecarenone into solid lipid nanoparticles. *Pharm. Res.* **2001**, *18*, 287–293.



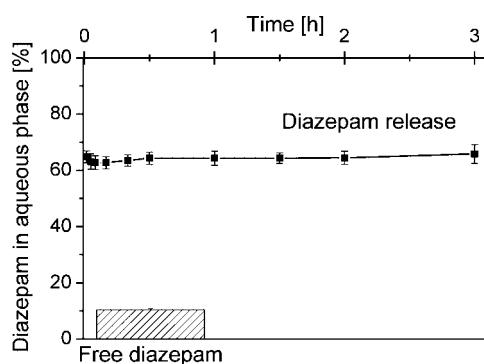


**Figure 7.** Release curve of a cold-stored tristearin dispersion containing 0.1% diazepam after dilution obtained with differential pulse polarography, and amount of diazepam in the water phase of the original dispersion determined with ultrafiltration ( $10.36 \pm 0.53\%$ ).

reflection of the freshly crystallized sample was of slightly higher intensity than that of the unloaded dispersion, whereas the size of the reflection obviously increased with time. The particle size remained almost constant during storage except for an outlier measured directly after preparation (Table 1).

The Q10-loaded dispersion stored at room temperature exhibited a larger fraction of  $\beta$ -polymorph already after preparation compared to unloaded or cold-stored Q10-containing dispersions. The size of this signal increased distinctly over storage time, in particular over the first 6 weeks. The  $\alpha$ -endotherm decreased slightly over time, while the size of the exotherm again almost remained constant and was only slightly higher than the exotherm of the cold-stored Q10-dispersion. Besides a rather high particle size measured after preparation (outlier), a small increase in particle size was observed after storage (Table 1).

**Drug Release.** The release of diazepam was investigated with differential pulse polarography, which was previously shown to be suitable for the measurement of drug release from lipid nanoparticles especially when using diazepam.<sup>33</sup>

Diazepam was released immediately after dilution without further increase over 3 h (Figure 7). The release was incomplete and remained at approximately 66%. Already in the undiluted dispersion, 10% of the total drug concentration was found in the aqueous phase.

## Discussion

**Characterization of Drug-Free Dispersions and Stability during Storage.** The use of PVA as emulsifier led to the formation of solid triglyceride nanoparticles from trimyrustin (cold-stored) and tristearin with mean particle sizes (PCS) in the range of about 140–165 nm after crystallization, which is in the common range of such kind of particles.

Compared to many other emulsifier compositions,<sup>25</sup> the use of PVA stabilized the nanoparticles in the metastable  $\alpha$ -modification. Only this polymorph was observed by X-ray diffraction in all dispersions directly after crystallization. Moreover, the  $\alpha$ -form was remarkably stable during storage. This particularly applied to tristearin nanoparticles for which

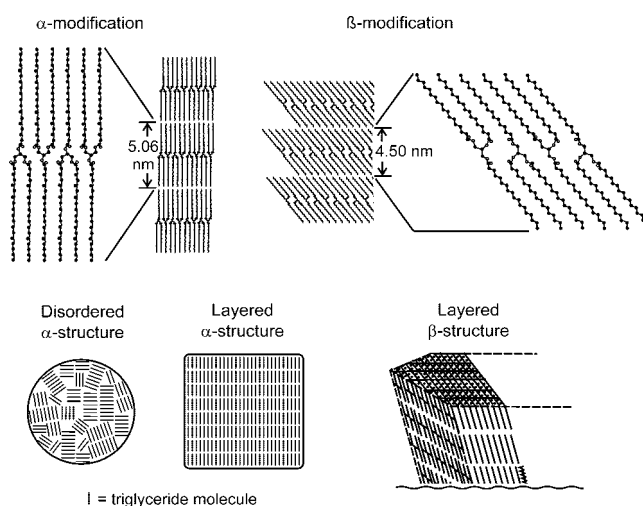


**Figure 8.** Schematic presentation of tristearin crystal structures. (Top) Molecular arrangement of the triglyceride in different polymorphs (modified after ref 44). (Bottom) Possible crystal structures of the  $\alpha$ -polymorph in the triglyceride nanoparticles as discussed in the text (left) and crystal of the  $\beta$ -polymorph (after refs 44 and 45) (right).

at most marginal alterations in the X-ray diffraction pattern and thermal behavior were observed during cold storage. As expected,<sup>16</sup> the use of higher storage temperatures (being closer to the  $\alpha$ -melting temperature) or the shorter chain triglyceride trimyrustin (which has a lower activation energy for the  $\alpha$ - to  $\beta$ -transformation in addition to a lower  $\alpha$ -melting temperature) reduced the stability of the  $\alpha$ -polymorph.

Although PVA-stabilized tristearin nanoparticles are clearly in the  $\alpha$ -modification according to their melting temperature and the position of the strong wide-angle X-ray reflection,<sup>11,38,39</sup> the structure of this  $\alpha$ -modification is unusual as it does not lead to a distinct small-angle reflection. Since the common molecular arrangement of triglycerides is lamellar (Figure 8), they cause small-angle reflections corresponding to their long spacings which depend on chain length and polymorphic form. The occurrence of only a very weak small-angle reflection in PVA-stabilized tristearin nanoparticles thus indicates the almost complete absence of a lamellar molecular order in these particles. Even though of similar (spherical) shape, the PVA-stabilized tristearin nanoparticles thus differ clearly from those stabilized with S100-3/SGC which were earlier found to be also quite stable in the  $\alpha$ -modification but which do contain lamellar ordering and do transfer slowly into the  $\beta$ -polymorph upon cold storage.<sup>10,36</sup> Concerning the almost complete absence of a small-angle reflection as well as their spherical shape and apparently unstructured core according to electron microscopic investigations, the structure of the PVA-stabilized tristearin nanoparticles in the  $\alpha$ -form resembles that of sodium glycocholate-stabilized

(38) Hoerr, C. W.; Paulicka, F. R. The role of X-ray diffraction in studies of the crystallography of monoacid saturated triglycerides. *J. Am. Oil Chem. Soc.* **1968**, *45*, 793–797.

(39) Larsson, K. Classification of glyceride crystal forms. *Acta Chim. Scand.* **1966**, *20*, 2255–2260.



tripalmitin nanoparticles obtained after rapid cooling.<sup>25</sup> For these tripalmitin nanoparticles, a mosaiclike internal structure consisting of high crystalline order among the fatty acid chains but low lamellar order of the single molecular layers has been proposed. A similar structure may also be assumed for the uncommon  $\alpha$ -modification observed in the present study (Figure 8). Completely different molecular arrangements may, however, also have to be taken into consideration. The glycocholate-stabilized tripalmitin nanoparticles mentioned above could only be brought into the “nonlamellar”  $\alpha$ -form under rapid cooling conditions, whereas the cooling conditions had almost no influence on the formation of the nonlamellar  $\alpha$ -form when PVA was used for the preparation of tristearin nanoparticles. This observation indicates that PVA is a better stabilizer for the nonlamellar  $\alpha$ -form than sodium glycocholate (although there may also be an influence of the triglyceride chain length). Tentatively, this might be due to either a much stronger effect or a different stabilization mechanism. Moreover, the  $\alpha$ -modification in solely sodium glycocholate-stabilized tripalmitin nanoparticles could “not be retained during extended storage”,<sup>25</sup> in contrast to the observations on the PVA-stabilized tristearin nanoparticles of the present study. While the thermal behavior of cold-stored PVA-stabilized tristearin nanoparticles remains almost unchanged over many months of storage, a slow increase in the recrystallization enthalpy is observed upon storage at room temperature over time. Since, under the same conditions, also the size of the small-angle reflection increases slightly (Figure 3), the increased recrystallization tendency might be correlated with an increase in lamellarity of the nanoparticles. A certain memory of triglyceride melts, for example, the preservation of lamellar structures in the liquid state as previously proposed,<sup>40–43</sup> might explain this correlation. If lamellar arrangements would still be present in the molten nanoparticles, this could favor recrystallization into the lamellar  $\beta$ -form upon heating. Indications that a higher degree of lamellarity in the  $\alpha$ -modification enhances transformation into the stable  $\beta$ -form have also been obtained in previous investigations on triglyceride nanoparticles,<sup>25,36</sup> but the effect remains to be investigated in more detail.

In contrast to the situation in tristearin nanoparticles, a high degree of lamellarity was found for cold-stored PVA-stabilized trimyristin nanoparticles by small-angle X-ray

diffraction. In electron microscopic investigations, the shape of these particles was more angular and thus closer to that of  $\beta$ -form nanoparticles. Some of the particles appeared circular in shape but did not display a denser inner structure which would point to a spherical shape as in the tristearin dispersion. Possibly, these particles exhibited a cylindrical shape as also observed for smectic cholesteryl myristate particles,<sup>8</sup> which could be projected in top view (circular) or in side view (more or less rectangular). At least some of the PVA-stabilized trimyristin nanoparticles in the  $\alpha$ -form seemed to reveal a layered structure in electron microscopy. According to the previously outlined hypothesis, a lamellar structure of the  $\alpha$ -polymorph should lead to a more rapid transformation into the stable  $\beta$ -form which was indeed observed here (but which may also be attributed to other causes outlined above). In spite of the more rapid transformation of PVA-stabilized trimyristin nanoparticles, even these particles could retain a large fraction of  $\alpha$ -modification upon cold storage for at least 9 months.

Although a large endotherm of the  $\beta$ -polymorph was observed in the thermograms of the cold-stored trimyristin dispersions, no reflections of the  $\beta$ -polymorph were observed in the wide-angle X-ray investigations. Obviously, a large fraction of the  $\beta$ -polymorph was formed during heating as reflected by the occurrence of a pronounced recrystallization exotherm. Since the exotherm is overlapping the endotherm of the  $\alpha$ -polymorph, the true amount of recrystallizing triglyceride might be larger than the evaluated amount. Moreover, a fraction of particles may already have transformed during sample preparation for DSC, as the  $\alpha$ -modification in trimyristin particles is rather instable at room temperature.

The reason for the high stabilization potential of PVA for the  $\alpha$ -polymorph of triglyceride nanoparticles is not yet clear. It has been observed earlier that PVA has a good stabilization potential for the supercooled and thus metastable thermotropic liquid crystalline smectic phase of cholesteryl myristate nanoparticles.<sup>8</sup>

In general, three effects of emulsifiers on the crystallization behavior can be observed in triglyceride nanoparticle dispersions:<sup>9,10,25,36</sup> They may have an impact on the crystallization temperature and mechanism, on the time-course of polymorphic transitions, and, at least for the  $\alpha$ -modification, on the structure of the formed crystals.

The crystallization of PVA-stabilized triglyceride nanoparticles occurs at very high supercooling typical of such nanoparticles. There is no indication for any crystallization enhancing effect of this emulsifier for the nanoparticles, which is in agreement with homogeneous nucleation, with no templating effect of the emulsifier.<sup>10</sup>

While crystallization is retarded in colloidal triglyceride particles, polymorphic transformations usually occur much faster than in the bulk material. This has been attributed to the small particle size leading to a high surface/volume ratio of the nanoparticles and to a high energy level and mobility of the

(40) Larsson, K. Molecular arrangement in glycerides. *Fette, Seifen, Anstrichm.* **1972**, 74, 136–142.

(41) Callaghan, P. T. The use of carbon-13 spin relaxation to investigate molecular motion in liquid tristearin. *Chem. Phys. Lipids* **1977**, 19, 56–73.

(42) Callaghan, P. T.; Jolley, K. W. Translational motion in the liquid phases of tristearin, triolein and trilinolein. *Chem. Phys. Lipids* **1980**, 27, 49–56.

(43) Sato, K. Solidification and phase transformation behaviour of food fats. A review. *Fett/Lipid* **1999**, 101, 467–474.

(44) Bunjes, H.; Unruh, T. Characterization of lipid nanoparticles by differential scanning calorimetry, X-ray and neutron scattering. *Adv. Drug Delivery Rev.* **2007**, 59, 379–402.

(45) Skoda, W.; Hoekstra, L. L.; Van Soest, T. C.; Bennema, P.; Van den Tempel, M. Structure and morphology of  $\beta$ -crystals of glyceryl tristearate. *Kolloid Z. Z. Polym.* **1967**, 219, 149–156.

triglyceride molecules at the nanoparticle surface.<sup>17,46</sup> Assuming that polymorphic transitions in triglyceride nanoparticles involve or are even initiated by molecular rearrangement processes at the particle surface, an influence of emulsifiers on the transformation is not surprising. It has indeed been shown that even very hydrophilic surfactants (e.g., the bile salt sodium glycocholate) which are supposed to be present only in the aqueous phase or at the particle interface can modify the polymorphism of triglyceride nanoparticles.<sup>25</sup> The comparatively slow transformation from the  $\alpha$ - to the  $\beta$ -form in triglyceride nanoparticles emulsified with the aid of saturated phospholipids (in combination with sodium glycocholate) has been attributed to a lack of mobility at the particle surface due to the presence of a rigid phospholipid "shell". In contrast, corresponding samples containing unsaturated phospholipids which are supposed to exhibit a high mobility of the more fluidlike fatty acid chains transform much faster from  $\alpha$  to  $\beta$ .<sup>10</sup> A trend toward promotion of  $\beta$ -modification formation in triglyceride nanoparticles was previously also observed for classic nonionic surfactants of lower molecular weight.<sup>25</sup> Although being a nonionic emulsifier as well, PVA does not follow this trend. Probably, PVA interacts with the particles in a different way because of its polymeric structure. One explanation might be that PVA causes a high viscosity or immobilization of the molecules in the interfacial region and therefore sterically hinders conformational reorientation of the molecules necessary for conversion from  $\alpha$  to  $\beta$ . As the transformation to the thermodynamically stable  $\beta$ -form does take place upon storage at higher temperatures, a kinetic stabilization is reasonable.

Maybe the most intriguing effect observed in the dispersions containing PVA is its strong effect on the structure of the  $\alpha$ -modification. The lack of lamellar order in the uncommon  $\alpha$ -polymorph may be involved in the good stabilization of the  $\alpha$ -modification in PVA-stabilized nanoparticles when assuming that a lamellar order is necessary for or facilitates the transformation to the  $\beta$ -polymorph as already outlined above. The common  $\alpha$ -polymorph (Figure 8) occurring in bulk triglycerides has a layered morphology and was also observed in slowly transforming colloidal triglycerides stabilized with saturated phospholipids or sodium glycocholate (slowly cooled).<sup>25,36</sup> For the latter nanoparticles, the cooling process determines the occurrence of the lamellar or the nonlamellar  $\alpha$ -form.<sup>25</sup>

In particles stabilized with PVA, the mechanism or the kinetics leading to the formation of the nonlamellar  $\alpha$ -form seems to be different, as the disordered structure was independent of the cooling conditions. PVA did not promote crystallization and nucleation; therefore, a mechanism based on a possible impact on crystal growth might be assumed. The crystal growth in triglycerides is usually controlled by surface kinetics leading to smooth crystal surfaces which

grow layer by layer.<sup>15,47</sup> Potentially, PVA inhibits the formation of a smooth surface at the lipid/PVA interface and/or favors the crystal growth away from the surface and with that promotes the formation of the less ordered structure. Moreover, a direct effect of PVA not only on the interface but also on the inner structure of the triglyceride particles cannot completely be ruled out.

Since these considerations are still very tentative, further investigations are required to clarify the exact cause for the very good stabilization of the  $\alpha$ -modification and especially the prevention of the formation of a long-range order of the triglyceride layers in the crystals in relation to structural elements of the emulsifiers or other substances such as drugs. Clarification of the underlying mechanisms may be particularly useful with respect to the observation that the presence of the nonlamellar  $\alpha$ -form might suppress the  $\alpha$ - to  $\beta$ -transformation.

**Storage at Elevated Temperatures/Influence of Crystallization Procedure.** In the previously cold-stored trimyristin dispersion stored at 23 °C (~9 °C below the melting onset of the  $\alpha$ -polymorph), a rapid transformation of nanoparticles from the  $\alpha$ - to the  $\beta$ -modification as revealed by DSC and X-ray diffraction was accompanied by a large increase in particle size and PDI. As it is known that triglyceride nanoparticles preferably assume the shape of more or less extended platelets,<sup>18,35</sup> this behavior may result from a rearrangement and change in the shape of the particles leading to the possibility of stronger interactions between the particles and/or a lack of emulsifier to stabilize the particle surfaces,<sup>48</sup> which might additionally agglomerate or aggregate during transformation especially in combination with the polymeric nature of the stabilizer. Cryoelectron microscopic investigations revealed an uncommon structure of the trimyristin particles in the  $\beta$ -form. Compared to solid trimyristin nanoparticles in the  $\beta$ -modification stabilized with natural soy bean lecithin and sodium glycocholate,<sup>18</sup> which exhibited a very thin plateletlike structure, the PVA-stabilized trimyristin particles in the  $\beta$ -polymorph showed a more cuboid structure with a much higher number of layers. The layers, however, exhibited several imperfections. The reason for the unusual structure remains to be clarified. It might result from the different stabilizer, for example, due to a high viscosity in the interfacial region as supposed above or be caused by the previously formed structure of the particles in the  $\alpha$ -modification from which it might not or only within much longer time be possible to form thin platelets.

Tristearin particles stored at 45 °C (i.e., 9 °C below the  $\alpha$ -polymorph melting temperature), which also transformed into the  $\beta$ -polymorph very rapidly, were less stable compared to the trimyristin dispersion stored at 23 °C during transformation from the  $\alpha$ - to the  $\beta$ -modification as reflected in a more distinct increase in particle size already observable

(46) Sonoda, T.; Takata, Y.; Ueno, S.; Sato, K. Effects of emulsifiers on crystallization behavior of lipid crystals in nanometer-size oil-in-water emulsion droplets. *Cryst. Growth Des.* **2006**, *6*, 306–312.

(47) Ghotra, B. S.; Dyal, S. D.; Narine, S. S. Lipid shortenings: a review. *Food Res. Int.* **2002**, *35*, 1015–1048.

(48) Westesen, K.; Siekmann, B. Investigation of the gel formation of phospholipid-stabilized solid lipid nanoparticles. *Int. J. Pharm.* **1997**, *151*, 35–45.

after 1 day. Tentatively, this behavior may be correlated with the tendency of tristearin nanoparticles to obtain a more anisometric shape in the  $\beta$ -modification than trimyristin nanoparticles.<sup>49</sup>

At 37 °C, the transformation into the  $\beta$ -polymorph was still rather fast and was again accompanied by a large increase in particle size.

Tristearin nanoparticles stored at 23 °C after crystallization in the refrigerator were much more stable than nanoparticles which were stored at that temperature directly after preparation without cold storage in between (Figure 2). The crystallization at refrigerator temperature seems therefore necessary for the formation of structures which are important for the stability. A reason for this might be the formation of a less well structured form of the  $\alpha$ -polymorph upon crystallization at lower temperature, although there was only a marginal effect of the crystallization conditions on the size of the small-angle reflection as discussed below. The DSC curves of the not previously cold-stored dispersion, however, do indicate a higher recrystallization tendency after melting of the  $\alpha$ -form than in the formerly cold-stored dispersion. Anyway, handling of a cold-stored tristearin dispersion for a few hours or even days at room temperature does not change the phase behavior significantly as also reflected in the minor changes in the small-angle X-ray diffraction pattern after 11 weeks of storage at 23 °C. This facilitates further investigation of these particles.

Previous investigations showed that the temperature program during crystallization may cause differences in the structure of the resulting particles in the  $\alpha$ -modification.<sup>25,36</sup> Therefore, the potential influence of the crystallization procedure of PVA-stabilized tristearin nanoparticles was investigated and was compared to tristearin nanoparticles stabilized with a mixture of hydrogenated soybean phospholipid (S100-3) (2.4%) and sodium glycocholate (0.6%) which has been described in ref 36.

The fact that the crystallization procedure or the cooling rate, respectively, have almost no effect on the formation and structure of the  $\alpha$ -polymorph in PVA-stabilized dispersions provides further evidence for the high stabilization potential of PVA on the  $\alpha$ -polymorph. The impact of the crystallization process is thus much lower than on the phospholipid-stabilized dispersion.

**Drug Loading.** Loading with diazepam showed almost no influence on the thermal behavior upon storage compared to the unloaded tristearin dispersions. One reason for that might be the low drug concentration in the dispersion.

As expected from the results of previous investigations,<sup>17,37</sup> the presence of Q10 (being incorporated in a much higher concentration than diazepam) led to the formation of higher fractions of the  $\beta$ -polymorph compared to the unloaded dispersion. To some extent, the reduced melting temperature of the  $\alpha$ -polymorph might be the cause of this. The Q10-loaded

dispersions also exhibited a reduction of the crystallization temperature, which was also seen in the diazepam-loaded dispersions, although to a smaller degree. The size of the recrystallization exotherm, however, remained almost constant during storage, whereas that of the room temperature stored unloaded and that of the diazepam dispersion increased over time. The reason for that behavior is, however, not yet clear.

**Drug Release.** Except for an incomplete drug release, there was no retardation in the release of diazepam from nanoparticles in the  $\alpha$ -modification. This is in good agreement with release results from various other colloidal dispersions such as, for example, emulsions of supercooled melts and solid triglyceride nanoparticles in the  $\beta$ -modification,<sup>32</sup> cubic phase nanoparticles,<sup>33</sup> or colloidal fat emulsions.<sup>50</sup> The burst release may be caused by a rather high mobility of the drug in the particles and/or the small particle size, that is, short diffusion pathways which do not slow down the release in a measurable way. Furthermore, the loading capacity of particles in the  $\alpha$ -modification may not be very high, leading to a large fraction of drug adsorbed to the particle surface. In this case, the drug would be “released” particularly fast into a large amount of release medium.

Assuming a partition controlled distribution of the drug during preparation, a partition coefficient of 1.93 ( $\log P$ ) can be calculated (based on a real drug concentration of 0.873 mg/mL, a real triglyceride concentration of 91.28 mg/mL, and 10.36% of the drug in the aqueous phase). From this value, it should be possible to calculate the theoretically expected amount of released drug upon a dilution of 1:101 when a partition controlled release is assumed as it was shown for cubic particles.<sup>33</sup> Such a calculation does, however, result in a much higher amount of released drug (92.8%) than it is observed in the experiment (~66%).

Hence, a partition control of the released drug fraction could not be shown here. Within the time scale of the experiment, the nanoparticles released a smaller amount of drug than would be expected from the partition coefficient. The question whether this indicates a very strong interaction of a certain fraction of drug with the nanoparticles or has to be attributed to other causes, for example, the method for measurement of the drug release, remains to be investigated in more detail.

## Conclusion

By using PVA as emulsifier, stable triglyceride nanoparticles in the  $\alpha$ -modification could be prepared. The dispersion of highest stability which was, therefore, investigated in most detail was a tristearin dispersion stored at refrigerator temperature with a PCS particle size of about 140 nm and a PDI of 0.15. It consisted of spherical particles as observed in transmission electron microscopy. Neither the crystallization procedure nor a short-term storage time at room temperature affected the stability of the  $\alpha$ -polymorph in this dispersion to a detectable extent. Furthermore, incorporation of drugs was possible while still retaining a large fraction of particles in the  $\alpha$ -modification. Whether the drug incorporation capacity of such nanoparticles in the  $\alpha$ -form is

(49) Illing, A.; Unruh, T. Investigation on the flow behavior of dispersions of solid triglyceride nanoparticles. *Int. J. Pharm.* **2004**, *284*, 123–131.

higher than that for nanoparticles in the stable  $\beta$ -modification remains to be investigated as does the drug release which was incomplete for the model drug diazepam after a large burst effect.

### Abbreviations Used

PVA, poly(vinyl alcohol); PDI, polydispersity index; DSC, differential scanning calorimetry; Dzp, diazepam; Q10, ubidecarenone; TM, trimyristin; TS, tristearin; HPLC, high performance liquid chromatography.

**Acknowledgment.** The authors gratefully acknowledge F. Steiniger and J. Thamm for the transmission electron microscopic investigations, A. Mohn for the help with the X-ray diffractometric measurements, and J. Kuntsche for providing drawings for Figure 8.

MP8000759

- 
- (50) Magenheimer, B.; Levy, M. Y.; Benita, S. A new in vitro technique for the evaluation of drug release profile from colloidal carriers. Ultrafiltration technique at low pressure. *Int. J. Pharm.* **1993**, *94*, 115–123.